ACS Sustainable Chemistry & Engineering

Research Article

pubs.acs.org/journal/ascecg

Synthesis and Enhanced Colloidal Stability of Cationic Gold Nanoparticles using Polyethyleneimine and Carbon Dioxide

Fiaz S. Mohammed, Scott R. Cole, and Christopher L. Kitchens*

Department of Chemical and Biomolecular Engineering, Clemson University, Clemson, South Carolina 29631, United States

Supporting Information

ABSTRACT: Employing green methods in the design and synthesis of functionalized metallic nanoparticles poses significant challenges in terms of maintaining product integrity (size, shape, dispersity, and colloidal stability). In this study, the direct synthesis of cationic gold nanoparticles (GNPs) capped by low molecular weight ($M_w \sim 600$) polyethylenimine was investigated. Specifically, three separate $HAuCl_4$ reduction pathways were used to produce robust GNPs with sizes ranging from 4 to 20 nm in diameter with excellent size control. The inclusion of carbon dioxide as a nontoxic, nonflammable, and inexpensive component led to decreases in particle size and an increase in the colloidal stability of the GNPs. Furthermore, the thermally reversible reaction of CO_2 with amines provides means to control the solvent pH through carbamate structures and, hence, the controllable formation of particle aggregates. The effects of pH, PEI concentration, and reduction method on the particle core size and stability were determined via transmission electron microscopy, UV−vis absorption spectra, and dynamic light scattering.

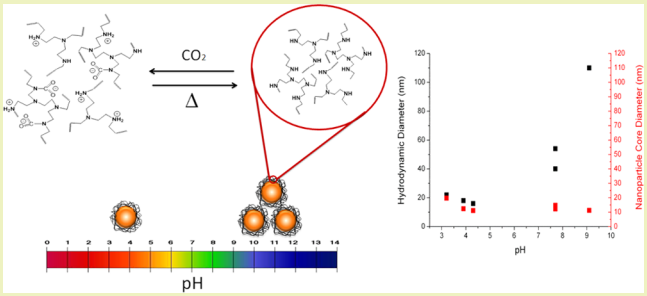

KEYWORDS: *Gold nanoparticles, PEI, Cationic, Carbamic acid*

INTRODUCTION

Gold nanoparticles (GNPs) possess unique size- and shape-dependent catalytic activity, optical properties, conductivities, and electron densities that have made their application highly attractive for both fundamental and applied sciences.[1,2] The use of surfactants, polymers, or other surface active ligands can be used to control the nanoparticle size, shape, and surface functionality, which in turn affects the nanoparticle's performance. The colloidal stability of these nanoparticles is also of significant importance and is achieved by using effective surface ligands. Furthermore, particle aggregation can significantly or irreversibly impair the performance of colloidal nanomaterials. For example, upon aggregation, the surface plasmon resonance for each GNP becomes delocalized, altering the optical properties. To alleviate this problem and enhance colloidal stability, the capping ligands can be designed to provide stability against exposure to salt, light, heat, and pH. This has led to numerous studies focused on tailoring and understanding the surface chemistry of colloidal nanomaterials for a diversity of applications.[3−6] By understanding the surface interactions, narrow particle size distributions can be synthesized with a high degree of nanoparticle stability. This in turn reduces not only the solvent and energy demand required for post-synthesis purification and fractionation but can also dictate the material fate and toxicity as well. As the field of nanotechnology expands, investigations into their physical and chemical properties along with environmental and health hazards have not proceeded at the same rate at which new materials are being produced. This was demonstrated with the rapid emergence and then decline of research focused on quantum dots as the potential toxicity of the materials led to the search of safer materials. Despite the growing awareness of nanomaterial toxicities, there is still enormous potential for creating greener methods of nanomaterial production that will have a decreased impact on human health and the environment.

One approach to mitigate the potential hazards of engineered colloidal nanomaterials is through the application of the 12 principles of green chemistry[7] that facilitate the reduction of hazardous chemical usage/generation from the design of the nanomaterials, which is a field known as green nanotechnology.[8] One example of greener nanoproduction methods is the use of polyelectrolytes to provide both steric and electrostatic stabilization of engineered colloidal nanomaterials.[9] Among these polyelectrolytes are cationic polymers such as polyethyleneimine (PEI), a highly branched polymer with a high pH-buffering capacity that is used in the biomedical field.[10−13] The positive surface charges of these nanoparticles play a vital role in determining the interactions with the charged moieties within cells and has been demonstrated to impact uptake in mammalian cells.[14−17] PEI has been used in the development of new DNA and gene transfection and delivery agents that exploits the cationic nature of the polymer

Special Issue: Sustainable Nanotechnology

Received: February 1, 2013
Revised: April 16, 2013
Published: May 8, 2013

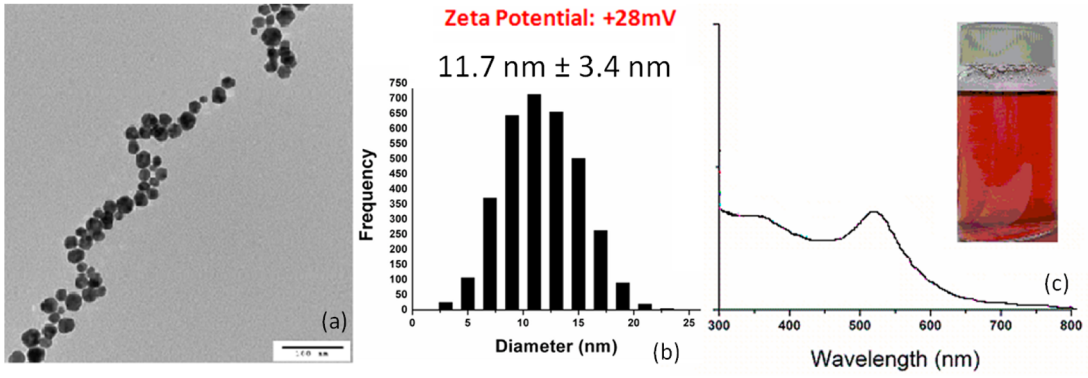

Figure 1. TEM image of PEI−GNPs (a) along with the corresponding particle size distribution histogram (b) and UV−vis absorption spectrum (c). Particles were synthesized via thermal reduction with 0.01 wt % PEI and a 1 min boiling time. The reported zeta potential is for a 15 min boiling time with 0.01 wt % PEI.

and attraction to the negatively charged phosphate backbone of the DNA.[18] Also, mathematical modeling has shown that the small cationic charges can lead to increases in transvascular flux of gold nanoparticles.[19] Additional biomedical applications of cationic nanoparticles range from targeted drug delivery to sensing, diagnostics, and imaging.[17,20−22]

Despite the numerous advantages of cationic nanomaterials, there are few studies that successfully synthesize positively charged gold nanoparticles as effectively as the more common anionic counterparts. The most direct method for cationic nanoparticle synthesis and functionalization involves a $NaBH_4$ reduction under solvent conditions. Lee et al.[23] synthesized 3−40 nm diameter cationic silver nanoparticles (SNPs) using molecular weight (M_w ~ 25,000) PEI and sodium borohydride ($NaBH_4$) as a reducing agent, while Schiffman et al.[24] synthesized 2.6 nm diameter SNPs capped with M_w ~ 2000 PEI and a $NaBH_4$ reduction method for application as a biocidal coating for modified polysulfone mats. Sun et al. demonstrated the reduction of both gold and silver metal precursors in the absence of external reducing agents, where the branched PEI acts as both the reducing and capping agent.[25−27] These studies do not address the need to produce particles of varying sizes and, more importantly, the effect of pH on the colloidal stability of the resulting nanoparticles. With respect to nanoparticle synthesis, a higher M_w PEI is preferred due to the increased colloidal stability, and there are a limited number of studies that use low M_w. High levels of PEI have also been shown to reduce the viability of cells, motivating the use of lower molecular weight PEI for in vivo studies.[28,29] To alleviate this trade-off between nanoparticle stability and cell viability, this work demonstrates the use of low M_w PEI, coupled with reversible carbamate formation, to promote and enhance nanoparticle stability. The reversible carbamate reaction uses CO_2, a safe and inexpensive additive that upon exposure with an amine, results in carbamic acid formation. This transformation has been exploited in the development of switchable surfactants,[30] reversible organogels,[31,32] supramolecular polymers,[33,34] hybrid organic−inorginc materials,[35] and dynamic surface coatings.[36] In each of these applications, the carbamate structures provide a reversible switch in both the physical and chemical properties of the amine, as well as a reversible switch in solvent pH.

This work demonstrates the use of low M_w PEI in the synthesis of cationic GNPs and examines the role of CO_2 and pH on the resulting particle core size and colloidal stability for three different methods of Au ion reduction, which include $NaBH_4$, thermal, and room-temperature reduction. The methods discussed in this paper are also extendable to silver nanoparticles; however, we have limited the scope to GNPs.

EXPERIMENTAL PROCEDURES

Materials. Hydrogen tetrachloroaurate (III) trihydrate ($HAuCl_4{\cdot}3H_2O$, 99.99%), branched polyelectrolyte polyethyleneimine (PEI) of M_w ~600, and reducing agent sodium borohydride ($NaBH_4$, 98%) were purchased from VWR and used as received. All glassware was carefully washed with "Aqua Regia" (3:1 conc. HCl:HNO_3) to remove any trace metal or organic impurities.

Synthesis. The gold nanoparticles (GNPs) were first synthesized by the reduction of Au^{3+} ions in an aqueous solution of PEI using sodium borohydride ($NaBH_4$) as a reducing agent. Briefly, 100 μL aliquot of a 0.05 M aqueous $HAuCl_4{\cdot}3H_2O$ solution along with 50−200 μL of a 2 wt % PEI (0.005−0.02 wt % solution) was added to 20 mL of deionized water (DI-H_2O) in a clean scintillation vial. Subsequently, 100 μL of a freshly prepared 0.05 M $NaBH_4$ solution was added to the vial and stirred for 15 min to allow for complete reduction and formation of GNPs. A rapid change in solution color from clear to light brown indicates the initial nanoparticle formation.

Thermal Reduction. For GNP synthesis by thermal reduction, 100 μL of 0.05 M HAuCl4 was dissolved in 20 mL of a 0.005−0.020 wt % PEI aqueous solution. The solution was brought to boil on a hot plate, and the reduction process was observed by the solution color evolution from yellow to orange to red. The nanoparticle solution continued to boil for a period not exceeding 15 min, while a loosely fitted cap ensured minimal solvent loss during the synthesis. All other parameters were held constant.

Room-Temperature Reduction. The same solution (0.25 mM $HAuCl_4$, 0.005−0.02 wt % PEI) previously mentioned was added to a clean scintillation vial and allowed to sit at room temperature and pressure without the addition of $NaBH_4$ or other external reducing agents. The formation of nanoparticles was evidenced by the gradual evolution of color in the solutions over a period of two weeks, and the particles were further characterized as formed.

The effect of pH and PEI−CO_2 on the synthesis of GNPs was examined by replacing the DI-H_2O with 1 mM HCl solutions and by reacting CO_2 with PEI solutions for 2 min to induce carbamate formation. A CO_2 tank fitted with a low pressure regulator was used to bubble CO_2 at a constant flow rate of 10 psig. PEI−CO_2 is used to denote PEI that has been reacted with CO_2 to produce the carbamate salt.

Characterization. UV−vis absorption spectra of the particle dispersions were measured using a Varian Cary 50 UV−vis-NIR spectrophotometer. Transmission electron microscopy (TEM) imaging was performed on a Hitachi 7600 with a 120 kV accelerating voltage. A glass nebulizer was used to aerosolize the nanoparticle

dx.doi.org/10.1021/sc400028t | ACS Sustainable Chem. Eng. 2013, 1, 826−832

dispersion for collection on 300 mesh-sized Formvar carbon-coated copper TEM grids (Ted Pella). The nanoparticle size distributions were obtained by image analysis with the ImageJ software counting at least 200 particles. Zeta-potential and dynamic light scattering (DLS) measurements were performed on a Malvern Zetasizer Nano-ZS (ZEN3600) at 25 °C with an incident wavelength of 633 nm and a 173° backscattering angle. One centimeter path length disposable zeta potential cells were rinsed with deionized water and loaded into the machine. The viscosity, refractive index, and absorption values were provided in the Malvern software for water (μ = 0.8872 cP, RI = 1.333) and crystalline gold (RI = 0.197, absorption = 3.091).

RESULTS AND DISCUSSION

The formation of gold nanoparticles (GNPs) was confirmed by the physical change in the reaction mixture from a clear solution to a colored colloidal dispersion. The color of the subsequent PEI–GNPs was dependent on the concentration and reduction method utilized. Figure 1 displays 11.7 ± 3.4 nm diameter PEI-stabilized GNPs (PEI–GNPs), determined by TEM. The particle dispersion possesses a characteristic surface plasmon resonance bands observed using UV–vis spectroscopy. This characteristic absorbance peak, observed at 524 nm, suggests that the PEI is an effective ligand for the synthesis and stabilization of colloidal GNPs. An absorption band at 360 nm is also observed in the UV–vis spectrum, which is attributed to the PEI.[37] This absorption was also found during this study when carbon dioxide was introduced to the PEI solution (Figure S9, Supporting Information). TEM images of the PEI–GNPs display a spherical shape and a monomodal distribution with relatively small standard deviations. The zeta potential of the PEI–GNPs synthesized by the three reduction methods all displayed positive ranges, which is consistent with a positively charged cationic ligand shell. More specifically, the PEI–GNPs that were thermally reduced (15 min) with 0.01 wt % PEI had a positive zeta potential of approximately +28 ± 11 mV. Hence, under aqueous conditions, the positively charged PEI provides colloidal stability due to the inherent electrostatic repulsion of the branched amino polymer.

Effect of Reduction Method. The reduction of the gold ions to metallic gold is the driving force behind nanoparticle nucleation and growth. It has been suggested that the formation of the PEI–GNPs in the absence of $NaBH_4$ is a product of the direct redox reaction between the PEI branches and the $HAuCl_4$.[38] Coordination between the amino groups with the metal ions results in the PEI acting as both a reductant and stabilizer, thus allowing the formation of the PEI–GNPs at room temperature in the absence of $NaBH_4$.

Figure 2 summarizes the nanoparticle core diameters determined by TEM analysis for particles synthesized using three reduction methods and three solvent conditions. There are significant differences in the GNP size among the three reduction methods, with average particle core diameters of 4.9 ± 1.3, 11.7 ± 3.6, and 17.7 ± 6.7 nm for the $NaBH_4$, thermal and room temperature methods respectively. A similar trend is observed in the UV–vis absorption maxima for the three methods, with average plasmon resonance bands centered at 510, 520, 527 nm, respectively. The UV–vis absorption peak maximum is directly related to the nanoparticle size, surface chemistry, and degree of clustering, where red shifting of the wavelength of maximum absorbance (λ_{max}) is indicative of increasing particle size and broadening of the spectra is associated with increasing polydispersity.[39] The observed trends are dictated by the reductive power of each reaction and the Au particle nucleation rate. The fastest reduction

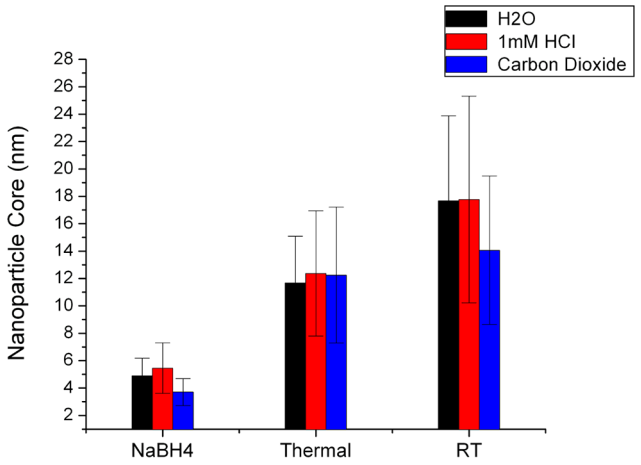

Figure 2. GNP mean core diameter determined by TEM for each reduction method using 0.01 wt %PEI with varying solvent conditions. The error bars represent the standard deviation of the particle size distribution for each sample population. Thermal boiling time = 1 min. Carbon dioxide = water + CO_2 bubbling (reduction of gold salt done at ambient pressure).

reaction uses an external chemical reducing agent, $NaBH_4$, and produces the smallest particles with the smallest size distribution. A trend of decreasing reduction rate and increasing particle size is demonstrated with thermal reduction followed by room-temperature reduction, as evidenced by both TEM and UV–vis absorption analysis.

Effect of Carbon Dioxide. Carbon dioxide readily reacts with amines to form a carbamic acid, which leads to a reduction in the pH of the resulting reaction solutions. Carbon dioxide is also well known to form carbonic acid in the presence of water, which also lowers the pH of the reaction solution. This reaction between the CO_2 and the polymer solution occurs very readily, and the time of carbon dioxide exposure does have an effect on the resulting pH of the PEI solution. An equilibrium pH of ~5 is obtained within 30 s of bubbling CO_2 at 10 psi through a 0.01 wt % PEI solution and is therefore not a variable in this study as all PEI solutions were exposed for a minimum of 2 min (Figure S3, Supporting Information). Furthermore, varying the PEI–CO_2 (polyethyleneimine that has been reacted with carbon dioxide) reaction sequence had minimal effect on the nanoparticle synthesis as evidenced by equivalent UV–vis absorption spectra regardless of the order in which the CO_2 is introduced. All combinations of introducing the starting materials (Au, PEI, and CO_2) into the reaction media were investigated (Figure S4,Supporting Information).

The presence of CO_2 in the synthesis of PEI-stabilized nanoparticles results in a decreased core diameter and size distribution of the nanoparticle produced by $NaBH_4$ reduction method from 4.9 ± 1.9 to 3.7 ± 1.0 nm. This decrease in core diameter is also evident in the UV–vis spectrum as the absorption peak at 503 nm, attributed to the 0.01 wt % PEI GNPs, is reduced to a shoulder as the CO_2 exposure increases (Figure 3). Furthermore, the effect of PEI concentration and CO_2 was observed visually as clustering and aggregation of the GNPs with 0.02 wt % PEI produced a dark black color, as compared to a lighter brown color for the 0.02 wt % PEI–CO_2 suggesting increased clustering in the former (Figure S5, Supporting Information).

Time-resolved UV–vis absorption studies of PEI–GNPs reduced at room temperature showed very good stability over a

dx.doi.org/10.1021/sc400028t | ACS Sustainable Chem. Eng. 2013, 1, 826–832

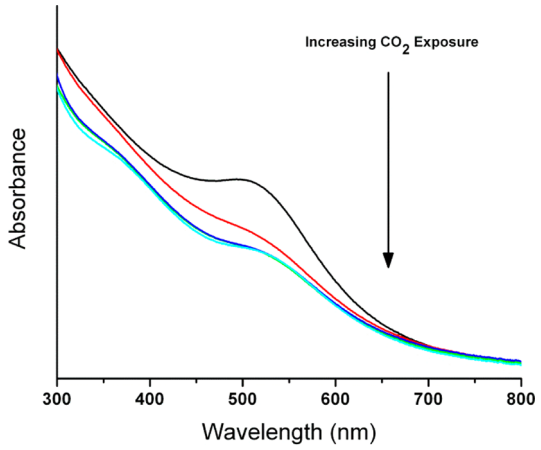

Figure 3. UV−vis absorption spectra of $NaBH_4$ reduced GNPs with increasing CO_2 exposure (over a 2 min period) prior to reduction at a PEI concentration of 0.01 wt %.

two week period, inferred from the stable plasmon resonance bands measured at 24 h intervals. The 0.005 wt % PEI and the 0.005 wt % PEI−CO_2 solutions showed an increase in maximum absorption over the entire two weeks, while the 0.01 wt % PEI−CO_2 exhibited a maximum absorption at day 7. The slower growth for the 0.005 wt % samples is likely a result of the decreased reductive power due to fewer PEI chains. The 0.02 wt % PEI solutions, due to clustering of the GNPs, displayed significant red shifting resulting in lower maximum absorbance, while the lack of red shifting for the 0.02 wt % PEI that was reacted with CO_2 (PEI−CO_2) further supports the addition of carbon dioxide as a stability enhancer with stable wavelengths of maximum absorbance over the time period. Overall, the GNPs wavelength of maximum absorbance remained constant (except for the 0.02 wt % in H2O) (Figures S7−S8, Supporting Information).

At an optimal concentration of 0.01 wt % PEI, TEM analysis of the thermally reduced PEI−GNPs determined that an increasing boiling time led to a 27% increase in particle core size from 11.7 ± 3.4 nm at 1 min to 14.8 ± 3.8 nm at 15 min (Figure 4). In addition, an increase in hydrodynamic radius (R_h) from 10.2 ± 3.5 to 34.1 ± 16.9 nm is observed for the same time intervals, indicating enhanced particle clustering at the longer boiling time.

The disparity in core size vs R_h at specific boiling times is observed further in Figure 5 as significant broadening and red shifting of the UV−vis absorption is attributed to particle

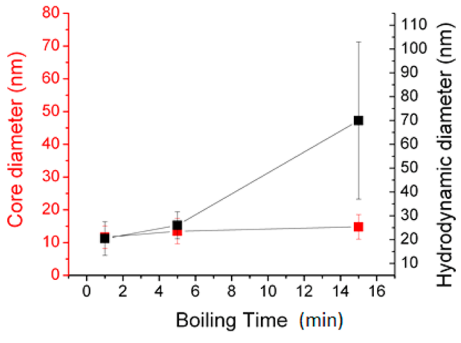

Figure 4. Graph of the thermally reduced 0.01 wt % PEI−GNPs in water core diameter (TEM) and hydrodynamic radius (DLS) vs boiling time (min).

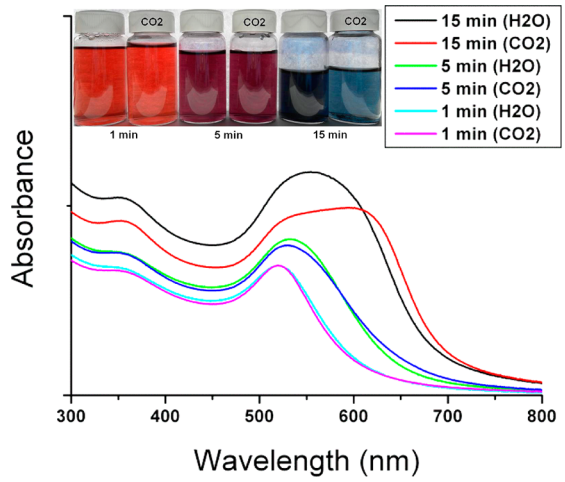

Figure 5. UV−vis absorption spectra of thermally reduced GNPs using 0.01 wt % PEI and 0.01 wt % PEI-CO_2 at 1, 5, and 15 min boiling times along with an image of the thermally reduced 0.01 wt % PEI GNPs at various boiling times. CO_2 = PEI−CO_2 solutions at ambient pressure.

clustering (Figure S6, Supporting Information, supports this conclusion as the GNPs boiled for 15 min are black in color). It is proposed that the low molecular weight PEI is degraded as the boiling time increases, leading to a diminished electrosteric stabilization potential of the polymer shell. This diminished polymer shell results in the increasing degree of clustering and thus larger R_h. The degradation is evidenced by a yellowing of the PEI solutions after thermal treatment and has been attributed to the formation of chromophores not present in pure PEI.[37] Because of the narrow size distributions, low hydrodynamic radii, and relatively stable particles obtained, the optimal boiling time for the conditions used in this study were determined to be 1 min with a PEI concentration of 0.01 wt %.

Unlike the $NaBH_4$ and ambient reduction method, the presence of CO_2 had little or no effect on the nanoparticles reduced by boiling (Figure 5). This is due to the thermally reversible carbamate chemistry that releases the gaseous CO_2 from the carbamate structures during the boiling process. Thus, CO_2 is not a suitable additive for stabilization during the thermal synthesis but can always be introduced post synthesis for increased electrostatic repulsion

The CO_2 reaction with the PEI and acidification of the nanoparticle suspensions synthesized by thermal reduction resulted in a reduced PEI−GNP hydrodynamic radius, determined by DLS (Table 1). This was more apparent at the higher concentrations of PEI, where we believe the electrosteric repulsions are more influential in providing colloidal stability. Upon heating, the reversibility of the CO_2−amine reaction returns the solvent properties to its original

Table 1. Hydrodynamic Radius (R_h) of GNPs Synthesized at 0.01 wt % PEI Concentration and Boiling Time of 1 min[a]

	thermally reduced PEI capped AuNPs		
	PEI	PEI+	thermal/nitrogen
mean Rh (nm)	20.6	13.3	17.3
std. dev. (nm)	4.8	2.7	4.3

[a]Nanoparticles had a stream of carbon dioxide bubbled through solution, followed by a thermal treatment with a nitrogen purge. PEI+ = PEI capped GNP solution after CO_2 addition.

dx.doi.org/10.1021/sc400028t | ACS Sustainable Chem. Eng. 2013, 1, 826−832

condition, evolving the CO_2. This reversal leads to the increase in R_h attributed to clustering of the nanoparticles as the repulsive forces are once again decreased. This result is significant as it highlights the potential of carbon dioxide as a green inexpensive additive to enhance colloidal gold stability post-synthesis, and it can replace the hazardous mineral acids as the pH adjuster.

Effect of PEI Concentration and pH. The electrostatic charge of the amino groups serves as one of the primary driving forces for reduction of the gold salt and particle stability following synthesis. As the PEI concentration increases, the greater number of PEI molecules can lead to decreased particle sizes as more molecules are readily available to cap the metallic core and suppress particle growth. At the same time, PEI can act as a reductant, where increased concentration would accelerate the nucleation and growth of the GNPs, producing larger particle cores and higher polydispersity when the PEI concentration is increased under neutral conditions.[23]

According to Table S1 of the Supporting Information, as the PEI concentration increased from 0.005 to 0.02 wt %, the synthesized GNP core size increased during the $NaBH_4$ reduction under neutral conditions from 4.6 ± 1.6 to 6.9 ± 2.9 nm. This agrees with the findings of Lee et al.[23] who attributed the dominant role of PEI as a reductant and the cause for the increased polydispersity and particle size. As expected, the R_h values also more than doubled when PEI concentration increased from 0.005 to 0.02 wt %, suggesting cluster formation. However, under acidic conditions (1 mM HCl), a decrease in diameter and size distribution was observed from 5.5 ± 2.5 to 4.9 ± 1.5 nm as PEI concentration increases (Figure S2, Supporting Information). It can be hypothesized that as the concentration of the PEI increases, the $NaBH_4$ rate of metal reduction decreases and results in larger particle cores. Furthermore, the Au^{3+} ion precursor may be more strongly chelated with the branched PEI and may not be as accessible when the $NaBH_4$ is introduced. Sun et al.[25,38] also mentions the formation of a polysalt between the nitrogen of a protonated amino dendrimer and the $HAuCl_4$. Hence, this can result in reduced nucleation of the Au ions and produce larger particles as the reduction time is increased.

For low pH conditions, the protonation of the PEI leads to an increase in electrostatic repulsion among branched PEI monomers, which produces an environment with increased ion mobility. This allows the $HAuCl_4$ to be dispersed more freely through the PEI solutions and allows the Au^{3+} ions to reduce more quickly by the $NaBH_4$, countering the effect of the increased hindrance at 0.02 wt % and producing smaller core size at 0.02 wt %. According to Figure 6, it is apparent that pH has an effect on the resulting UV−vis absorption bands of the GNPs reduced via $NaBH_4$. As the concentration of PEI increases from 0.005 to 0.01 and 0.02 wt %, the pH of the polymer solution increases from 4.3 to 7.1 and 9.1, respectively. The PEI particles synthesized at 0.005 wt % PEI and 0.01 wt % with a low pH (1 mM HCl solvent conditions) exhibit slight shoulders at 520 nm attributed to the NPs, while the 0.02 wt % PEI in H_2O exhibits an intense broad peak at 534 nm. The 0.02 wt % PEI in 1 mM HCl and the 0.01 wt % PEI in H_2O exhibit almost identical spectra with maximum absorption at wavelength 512 nm. This supports our theory that a reduced pH environment promotes faster reduction of the Au precursor and smaller particle cores despite a higher PEI concentration. This is attributed to their similarity in pH, which are 7.7 and 7.1, respectively, indicating that the concentration is responsible for adjusting the pH rather than impacting the resulting particle stability.

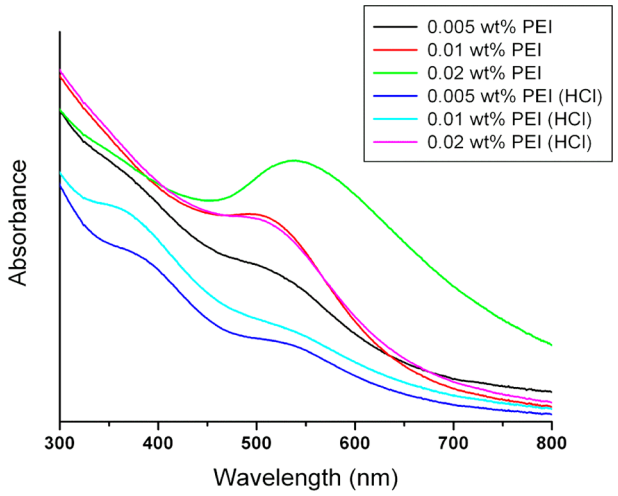

Figure 6. UV−vis absorption spectra of $NaBH_4$ reduced GNPs using 0.005−0.02 wt % PEI solutions in pure DI-H_2O and 1 mM HCl.

The thermal reduction is also affected by the pH of the PEI solution as shown in Figure 7. The GNPs synthesized in low pH environments exhibit sharp plasmon resonance bands indicating well-dispersed particles and minimal clustering, while a pH of 9.1 and 7.7 show a significant red shift and broadening of the UV−vis spectra.

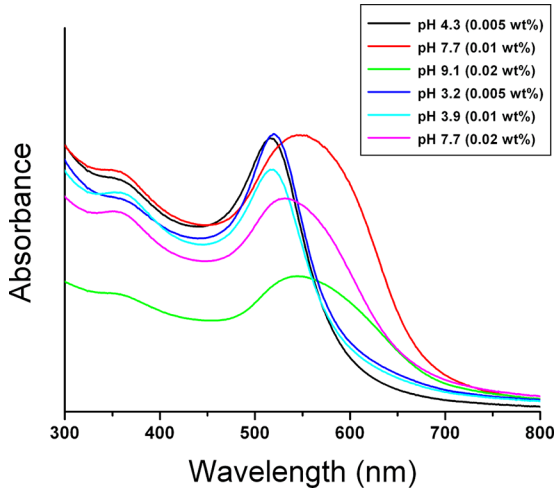

Figure 7. UV−vis absorption spectra of GNPs reduced using the thermal method using 0.005−0.02 wt % PEI in 1 mM HCl and DI-H_2O.

This is once again characteristic of polydispersity due to clustering or increased core sizes. Coupled with Figure 8, a better understanding of the effect of pH on the interparticle stability is gained. As the pH increases from 3.2 to 9.1, so does the hydrodynamic diameter of all the GNPs, while the core sizes remain relatively low. This trend further promotes the claim of increased clustering at the higher PEI concentrations, which can be mitigated through the acidification of the solvent and PEI protonation.

Likewise, the formation and growth of the PEI−GNPs synthesized by room-temperature reduction are also enhanced at a lower pH with the use of 1 mM HCl. After only 2 h, the

dx.doi.org/10.1021/sc400028t | ACS Sustainable Chem. Eng. 2013, 1, 826−832

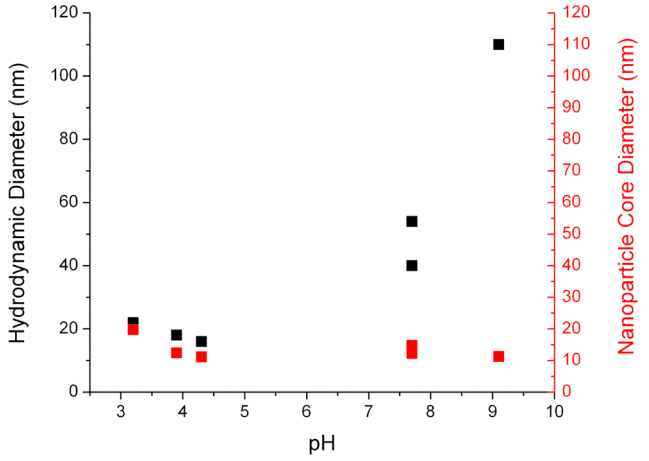

Figure 8. Graph of the core diameter (TEM) and hydrodynamic diameter (DLS) of thermally reduced GNPs vs pH. GNPs were synthesized using 0.005, 0.01, and 0.02 wt % PEI in 1 mM HCl and DI-H_2O.

Plasmon resonance bands of the GNPs can be detected under acidic conditions. However, there is a concentration limitation evident when comparing the two 0.005 wt % reactions. The particles synthesized at the lower pH (3.4) grow slower than those at pH 4.2, while the increase in PEI concentration to 0.01 wt % leads to faster reduction of the Au and hence a quicker growth in the UV−vis absorption when compared to 0.005 wt %. (Figure 9)

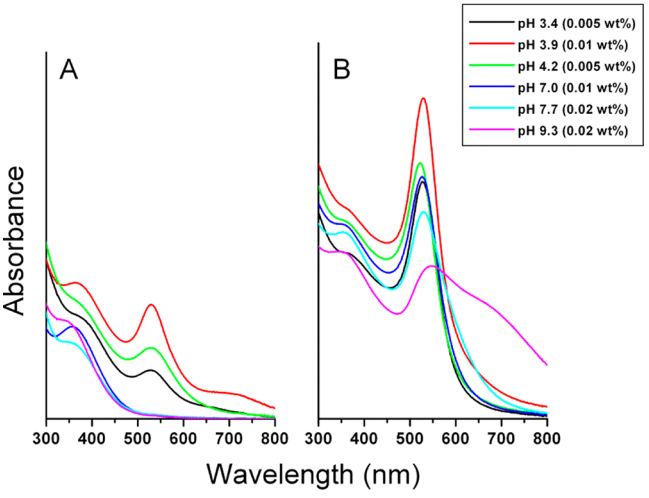

Figure 9. UV−vis absorption spectra of GNPs reduced at room temperature and pressure using various concentrations of PEI in 1 mM HCl and DI-H_2O after (A) 2 h and (B) 2 weeks.

After two weeks, UV−vis suggests that under basic conditions the GNPs are highly clustered and polydispersed. It is important to note that the PEI−GNPs synthesized at pH 9.3 and 7.7 have the same PEI concentration, which further supports our claim that electrosteric stabilization due to protonation of the amines is the driving force behind this particle stability. Hence, pH has a major effect on the particle UV−vis absorption of the GNPs, which is independent of reduction source.

CONCLUSIONS

Cationic gold nanoparticles were consistently synthesized using a low molecular weight (M_w ~ 600) polyethylenimine as the stabilizing ligand with three varying reduction methods. The pH of the synthesis was determined as a driving force for the reduction and stabilization of the PEI-capped GNPs that can be manipulated using traditional mineral acids or carbamate formation from a safe, cheap, and reversible reaction with carbon dioxide. The PEI−GNPs had a positive zeta potential of approximately +30 mV on average and formed stable colloidal suspensions through the increased electrostatic repulsion caused by CO_2 addition. At low PEI concentrations, the reduction in pH led to a slight increase in particle core size. However, there was a significant reduction in particle clustering as pH decreased. Overall, the addition of carbon dioxide as a greener pH adjuster improved the stability of PEI-capped gold nanoparticles by providing improved electrostatic repulsion due to reversible carbamate chemistry. This was determined from the hydrodynamic radii of the GNPs synthesized along with the positive zeta potentials obtained. Finally, the presence of CO_2 resulted in slightly smaller particle cores at room temperature and $NaBH_4$ reduction methods. This work sheds light on the ability of CO_2 to effectively stabilize cationic gold nanoparticles and its implementation in future green nanofabrication processes.

ASSOCIATED CONTENT

Supporting Information

Information as mentioned in the text. This material is available free of charge via the Internet at http://pubs.acs.org.

AUTHOR INFORMATION

Corresponding Author

*E-mail: ckitche@clemson.edu.

Notes

The authors declare no competing financial interest.

REFERENCES

(1) Shan, J.; Tenhu, H. Recent advances in polymer protected gold nanoparticles: Synthesis, properties and applications. *Chem. Commun.* **2007**, 4580−4598.

(2) Wang, J.; Wang, L.; Liu, X.; Liang, Z.; Song, S.; Li, W.; Li, G.; Fan, C. A gold nanoparticle-based aptamer target binding readout for ATP assay. *Adv. Mater.* **2007**, *19*, 3943−3946.

(3) Caragheorgheopol, A.; Chechik, V. Mechanistic aspects of ligand exchange in Au nanoparticles. *Phys. Chem. Chem. Phys.* **2008**, *10*, 5029−5041.

(4) Gittins, D. I.; Susha, A. S.; Schoeler, B.; Caruso, F. Dense nanoparticulate thin films via gold nanoparticle self-assembly. *Adv. Mater.* **2002**, *14*, 508−512.

(5) Hostetler, M. J.; Wingate, J. E.; Zhong, C.-J.; Harris, J. E.; Vachet, R. W.; Clark, M. R.; Londono, J. D.; Green, S. J.; Stokes, J. J.; Wignall, G. D.; Glish, G. L.; Porter, M. D.; Evans, N. D.; Murray, R. W. Alkanethiolate gold cluster molecules with core diameters from 1.5 to 5.2 nm: Core and monolayer properties as a function of core size. *Langmuir* **1998**, *14*, 17−30.

(6) Tao, K.; Jie, Z.; Jing, Y.; Yao, Y.; Xiaoping, W.; Pen, L.; Yang, A.; Roa, W.; Xing, J.; Jie, C.: Surface Modifications of Gold-Nanoparticles to Enhance Radiation Cytotoxicity. Life Science Systems and Applications Workshop, 2007. LISA 2007, IEEE/NIH, November 8−9, 2007; pp 265−268.

(7) Allen, D. T.; Shonnard, D. *Green Engineering: Environmentally Conscious Design of Chemical Processes*; Prentice Hall: Upper Saddle River, NJ, 2002.

(8) Hutchison, J. E. Greener nanoscience: A proactive approach to advancing applications and reducing implications of nanotechnology. *Acs Nano* **2008**, *2*, 395−402.
(9) Youk, J. H.; Locklin, J.; Xia, C. J.; Advincula, R.; Park, M. K. Preparation of gold nanoparticles from a polyelectrolyte complex solution of terthiophene amphiphiles. *Abstr. Pap., Am. Chem. Soc.* **2001**, *222*, U389−U389.
(10) De, l. O.; Matias, M. C.; Urreaga, J. M. Spectroscopic study of the modification of cellulose with polyethylenimines. *J. Appl. Polym. Sci.* **2004**, *92*, 2196−2202.
(11) Erbacher, P.; Bettinger, T.; Belguise-Valladier, P.; Zou, S.; Coll, J.-L.; Behr, J.-P.; Remy, J.-S. Transfection and physical properties of various saccharide, poly(ethylene glycol), and antibody-derivatized polyethylenimines (PEI). *J. Gene Med.* **1999**, *1*, 210−222.
(12) Shvero, D. K.; Davidi, M. P.; Weiss, E. I.; Srerer, N.; Beyth, N. Antibacterial effect of polyethyleneimine nanoparticles incorporated in provisional cements against *Streptococcus mutans*. *J. Biomed. Mater. Res., Part B* **2010**, *94B*, 367−371.
(13) Tang, M. X.; Szoka, F. C. The influence of polymer structure on the interactions of cationic polymers with DNA and morphology of the resulting complexes. *Gene Ther.* **1997**, *4*, 823−832.
(14) Zhou, Y. B.; Tang, Z. M.; Shi, C. L.; Shi, S.; Qian, Z. Y.; Zhou, S. B. Polyethylenimine functionalized magnetic nanoparticles as a potential non-viral vector for gene delivery. *J. Mater. Sci.: Mater. Med.* **2012**, *23*, 2697−2708.
(15) Zhao, Y.; Tian, Y.; Cui, Y.; Liu, W.; Ma, W.; Jiang, X. Small molecule-capped gold nanoparticles as potent antibacterial agents that target gram-negative bacteria. *J. Am. Chem. Soc.* **2010**, *132*, 12349−12356.
(16) Chakraborti, S.; Joshi, P.; Chakravarty, D.; Shanker, V.; Ansari, Z. A.; Singh, S. P.; Chakrabarti, P. Interaction of polyethyleneimine-functionalized ZnO nanoparticles with bovine serum albumin. *Langmuir* **2012**, *28*, 11142−11152.
(17) Saha, K.; Kim, S. T.; Yan, B.; Miranda, O. R.; Alfonso, F. S.; Shlosman, D.; Rotello, V. M. Surface functionality of nanoparticles determines cellular uptake mechanisms in mammalian cells. *Small* **2013**, *9*, 300−305.
(18) McBain, S. C.; Yiu, H. H. P.; El Haj, A.; Dobson, J. Polyethyleneimine functionalized iron oxide nanoparticles as agents for DNA delivery and transfection. *J. Mater. Chem.* **2007**, *17*, 2561−2565.
(19) Stylianopoulos, T.; Soteriou, K.; Fukumura, D.; Jain, R. K. Cationic nanoparticles have superior transvascular flux into solid tumors: Insights from a mathematical model. *Ann. Biomed. Eng.* **2013**, *41*, 68−77.
(20) Railsback, J. G.; Singh, A.; Pearce, R. C.; McKnight, T. E.; Collazo, R.; Sitar, Z.; Yingling, Y. G.; Melechko, A. V. Weakly charged cationic nanoparticles induce DNA bending and strand separation. *Adv. Mater.* **2012**, *24*, 4261−+.
(21) Popescu, M. T.; Tsitsilianis, C. Controlled delivery of functionalized gold nanoparticles by pH-sensitive polymersomes. *ACS Macro Lett.* **2013**, *2*, 222−225.
(22) Fleischer, C. C.; Payne, C. K. Nanoparticle surface charge mediates the cellular receptors used by protein-nanoparticle complexes. *J. Phys. Chem. B* **2012**, *116*, 8901−8907.
(23) Lee, H. J.; Lee, S. G.; Oh, E. J.; Chung, H. Y.; Han, S. I.; Kim, E. J.; Seo, S. Y.; Do Ghim, H.; Yeum, J. H.; Choi, J. H. Antimicrobial polyethyleneimine-silver nanoparticles in a stable colloidal dispersion. *Colloids Surf., B* **2011**, *88*, 505−511.
(24) Schiffman, J. D.; Wang, Y.; Giannelis, E. P.; Elimelech, M. Biocidal activity of plasma modified electrospun polysulfone mats functionalized with polyethyleneimine-capped silver nanoparticles RID B-4547-2010. *Langmuir* **2011**, *27*, 13159−13164.
(25) Sun, X. P.; Dong, S. J.; Wang, E. K. One-step synthesis and characterization of polyelectrolyte-protected gold nanoparticles through a thermal process. *Polymer* **2004**, *45*, 2181−2184.
(26) Sun, X. P.; Dong, S. J.; Wang, E. K. One-step preparation of highly concentrated well-stable gold colloids by direct mix of polyelectrolyte and HAuCl4 aqueous solutions at room temperature. *J. Colloid Interface Sci.* **2005**, *288*, 301−303.
(27) Sun, X. P.; Dong, S. J.; Wang, E. K. One-step polyelectrolyte-based route to well-dispersed gold nanoparticles: Synthesis and insight. *Mater. Chem. Phys.* **2006**, *96*, 29−33.
(28) Abdallah, B.; Hassan, A.; Benoist, C.; Goula, D.; Behr, J. P.; Demeneix, B. A. A powerful nonviral vector for in vivo gene transfer into the adult mammalian brain: Polyethylenimine. *Hum. Gene Ther.* **1996**, *7*, 1947−1954.
(29) Deng, R.; Yue, Y.; Jin, F.; Chen, Y.; Kung, H.-F.; Lin, M. C. M.; Wu, C. Revisit the complexation of PEI and DNA: How to make low cytotoxic and highly efficient PEI gene transfection non-viral vectors with a controllable chain length and structure? *J. Controlled Release* **2009**, *140*, 40−46.
(30) Jessop, P. G.; Heldebrant, D. J.; Li, X.; Eckertt, C. A.; Liotta, C. L. Green chemistry: Reversible nonpolar-to-polar solvent. *Nature* **2005**, *436*, 1102−1102.
(31) George, M.; Weiss, R. G. Chemically reversible organogels via "latent" gelators. Aliphatic amines with carbon dioxide and their ammonium carbamates. *Langmuir* **2002**, *18*, 7124−7135.
(32) George, M.; Weiss, R. G. Primary alkyl amines as latent gelators and their organogel adducts with neutral triatomic molecules. *Langmuir* **2003**, *19*, 1017−1025.
(33) Xu, H.; Rudkevich, D. M. CO_2 in supramolecular chemistry: Preparation of switchable supramolecular polymers. *Chem.—Eur. J.* **2004**, *10*, 5432−5442.
(34) Xu, H.; Rudkevich, D. M. Reversible chemistry of CO_2 in the preparation of fluorescent supramolecular polymers. *J. Org. Chem.* **2004**, *69*, 8609−8617.
(35) Alauzun, J.; Besson, E.; Mehdi, A.; Reyé, C.; Corriu, R. J. P. Reversible covalent chemistry of CO_2: An opportunity for nano-structured hybrid organic−inorganic materials. *Chem. Mater.* **2007**, *20*, 503−513.
(36) Mohammed, F. S.; Wuttigul, S.; Kitchens, C. L. Dynamic surface properties of amino-terminated self-assembled monolayers incorporating reversible CO_2 chemistry. *Ind. Eng. Chem. Res.* **2011**, *50*, 8034−8041.
(37) De La Orden, M. U.; Matías, M. C.; Martínez Urreaga, J. Spectroscopic study of the modification of cellulose with polyethylenimines. *J. Appl. Polym. Sci.* **2004**, *92*, 2196−2202.
(38) Sun, X. P.; Jiang, X.; Dong, S. J.; Wang, E. K. One-step synthesis and size control of dendrimer-protected gold nanoparticles: A heat-treatment-based strategy. *Macromol. Rapid Commun.* **2003**, *24*, 1024−1028.
(39) Link, S.; El-Sayed, M. A. Size and temperature dependence of the plasmon absorption of colloidal gold nanoparticles. *J. Phys. Chem. B* **1999**, *103*, 4212−4217.

NOTE ADDED AFTER ASAP PUBLICATION

This article was published ASAP on May 29, 2013, with an error in the Abstract and Table of Contents graphics. The corrected version was published ASAP on June 19, 2013.